



A photochemical approach for controlled drug release in targeted drug delivery

Seok Ki Choi^{a,b,*}, Manisha Verma^c, Justin Silpe^c, Ryan E. Moody^d, Kenny Tang^c, Jeffrey J. Hanson^c, James R. Baker Jr.^{a,b,*}

^a Michigan Nanotechnology Institute for Medicine and Biological Sciences, University of Michigan, Ann Arbor, MI 48109, USA

^b Department of Internal Medicine, University of Michigan, Ann Arbor, MI 48109, USA

^c College of Literature, Science and The Arts, University of Michigan, Ann Arbor, MI 48109, USA

^d College of Engineering, University of Michigan, Ann Arbor, MI 48109, USA

ARTICLE INFO

Article history:

Received 26 October 2011

Revised 6 December 2011

Accepted 13 December 2011

Available online 20 December 2011

Keywords:

o-Nitrobenzyl linker

Photocleavage

Methotrexate

Dendrimer

Controlled release

Drug delivery

ABSTRACT

Photochemistry provides a unique mechanism that enables the active control of drug release in cancer-targeting drug delivery. This study investigates the light-mediated release of methotrexate, an anticancer drug, using a photocleavable linker strategy based on *o*-nitrobenzyl protection. We evaluated two types of the *o*-nitrobenzyl-linked methotrexate for the drug release study and further extended the study to a fifth-generation poly(amidoamine) dendrimer carrier covalently conjugated with methotrexate via the *o*-nitrobenzyl linker. We performed the drug release studies by using a combination of three standard analytical methods that include UV/vis spectrometry, ¹H NMR spectroscopy, and anal. HPLC. This article reports that methotrexate is released by the photochemical mechanism in an actively controlled manner. The rate of the drug release varies in response to multiple control parameters, including linker design, light wavelength, exposure time, and the pH of the medium where the drug release occurs.

© 2011 Elsevier Ltd. All rights reserved.

1. Introduction

Targeted delivery plays an essential role in the detection, diagnosis and treatment of life-threatening diseases, including cancers.^{1–3} A challenging aspect facing the delivery strategy relates to the timely control of the drug release after uptake by the targeted cell.^{1,4–7} Most of the release mechanisms currently being explored involve chemical and enzymatic reactions which are triggered passively under the influence of specific internal cellular factors (Fig. 1). We have been interested in designing an orthogonal release approach in which an external tool such as light^{8–13} or ultrasound^{14,15} is applied to actively trigger the drug release. The present study aims to investigate a photon-based external approach for the release of methotrexate (MTX) as the model cancer drug.

MTX belongs to a class of antifolate molecules and constitutes one of the clinically approved anticancer drugs.^{1,16,17} It is a potent inhibitor ($K_i = 0.058 \text{ nM}^{16}$) of dihydrofolate reductase (DHFR^{18,19}) localized in the cytoplasm. Despite its proven therapeutic value in the treatment of certain cancers²⁰ and rheumatoid arthritis,²¹ MTX suffers from its non-selective cytotoxicity that contributes to lower its therapeutic index.¹⁷ As the approach frequently applied

to overcome such a therapeutic limitation, targeted delivery provides a route for facilitating the MTX uptake by a cancer cell, and as a consequence, for enhancing its therapeutic index.^{4,6,7,22} This

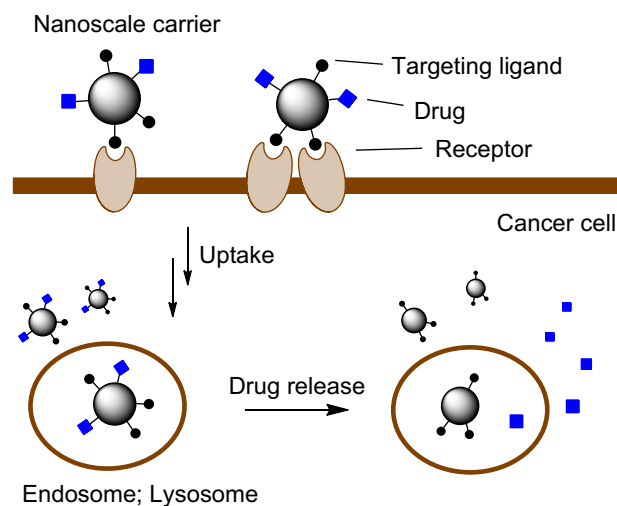


Figure 1. A proposed schematic illustrating the concept of cancer targeting drug delivery. The drug release can be controlled by the mechanism triggered by an endogenous factor (low pH, reduction, enzymes), or an external tool such as light.

* Corresponding authors. Tel.: +1 734 615 0618; fax: +1 734 615 0621 (S.K.C.); tel.: +1 734 647 2777; fax: +1 734 615 2990 (J.R.B.).

E-mail addresses: skchoi@umich.edu (S.K. Choi), jrbakerjr@umich.edu (J.R. Baker).

strategy relies on a macromolecular system designed in a rational way such that the therapeutic payloads are carried by a system that is conjugated with a targeting ligand for binding to the cancer cell.^{5,6,23–27} Such delivery strategy has already led to a number of successful applications for MTX^{5,28} and for other anti-cancer therapeutic agents represented by cisplatin,⁶ doxorubicin,²⁹ and paclitaxel.^{4,23} In each of these cases, the drug molecule is delivered by a nanometer-sized carrier based on dendritic macromolecules,²² liposomes,³⁰ polymers,³ and metallic nanoparticles.⁶ Despite the rapid progress achieved in this field, there are certain technical aspects that deserve further optimization—in particular, in the method of drug release. Most of the current release methods rely on either a chemical or enzymatic cleavage reaction of the linker that tethers the drug molecule.^{4,6,7} Such methods are incorporated by an ester-based or amide-based linker which is cleaved hydrolytically at the acidic subcellular compartments, such as the endosomes and lysosomes (pH 4–5), where the drug carriers are internalized.^{6,7} In addition, there are other specialized linkers based on di-sulfide,⁴ indolequinone,³¹ and nitroheterocycle³² which are cleavable differently through bioreductive mechanisms. Despite the differences among such release mechanisms, it is common that the drug release occurs passively only in response to environmental and pathophysiological factors.

This study aims to investigate the orthogonal method, which allows the active release of drug molecules through application of an external trigger. We employed photochemistry as the orthogonal means to control the release of MTX. Our approach is based on the concept of photocaging,³³ in which a biologically active molecule (ligand, drug) is temporarily inactivated by protecting it with a photocleavable group ('photocaged'). This caged molecule releases its parent species in an actively controlled manner only when its photosensitive protective group is cleaved by UV irradiation. The focus of this release method has mainly been on chemical and biological problems, such as the spatiotemporal control of cell signaling processes,^{34–36} and it was only recently applied to drug delivery.^{8,11–13} The photocleavable linkers that are applicable for the current application are comprised of those based on *o*-nitrobenzyl (ONB),^{33,35,37} coumarin,^{35,36} xanthene,³⁸ and benzophenone.³⁹ Figure 2 illustrates a schematic for controlled drug release triggered by a photochemical mechanism where a drug molecule attached to the photocleavable linker is released upon UV irradiation.⁸ In the present study, we selected the ONB group as the core of the photocleavable linker and developed linker chemistry that is applicable for the drug attachment and conjugation to poly(amidoamine) (PAMAM) dendrimer as the delivery platform. Here, we report the photochemical mechanism of MTX release with the ONB-linker strategy and analyze a set of key basic parameters that determine the kinetics of the drug release.

2. Results and discussion

2.1. Design of methotrexate (MTX)-photolinker conjugates

The two photolinker molecules **1** and **2** used in this study are shown in Figure 3. The core of each linker is based primarily on the ONB group,^{40–42} where its benzylic alcohol serves as the photolabile site for its covalent conjugation with an MTX molecule. The structure of each linker also contains a primary amine located at the end opposite to the benzylic position, and this terminal amine serves as the site to covalently anchor the photocaged drug molecule to a PAMAM dendrimer carrier. The two linkers are quite homologous in their structure and bifunctional design, but they are different in the pattern of aromatic substitutions at the ONB group. We introduced such variation in order to evaluate the significance of the ONB core in the photochemical drug release and to identify an optimal substitution pattern for the ONB core.

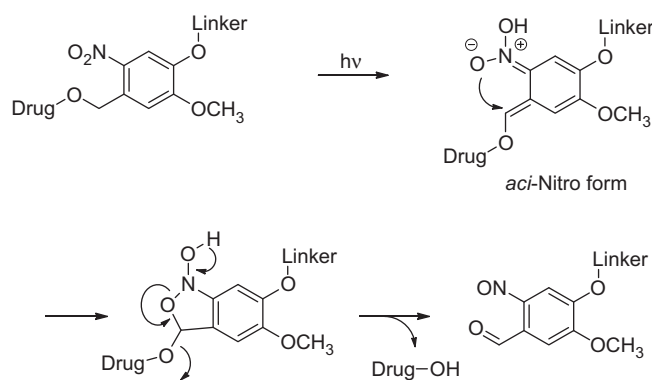


Figure 2. A schematic for photon-based cleavage of an *o*-nitrobenzyl (ONB) linker as the mechanism that enables the controlled drug release.

A synthetic method for photolinker **1** and its MTX conjugate **3** is described in Scheme 1. Synthesis of **1** was achieved by the *O*-alkylation reaction of 2-nitro-5-hydroxybenzyl alcohol with a bromoacetamide-containing spacer, **6**. The linker **1** was then derivatized to **7** by reacting with bromoacetyl chloride such that its resultant bromoacetate moiety is used for the conjugation with MTX by the *O*-alkylation reaction at the carboxylate site of the L-glutamate domain. After the coupling reaction, the product **8** was isolated by flash silica column chromatography as a mixture of two regioisomers, α - and γ -ester ($\alpha/\gamma = 37/63$ on the basis of ¹H NMR data; only the γ -isomer is shown). Their separation was not attempted because each isomer is able to release the MTX payload. The *N*-Boc group in **8** was deprotected by the TFA treatment, yielding a MTX-linker **3** that contains a free primary amine at the linker terminus.

Synthesis of the other MTX-linker **4** was completed by adopting the synthetic approach as described earlier but with minor modifications (Scheme 2). In this synthetic process, the benzyl alcohol of the linker **2** was preactivated to its methanesulfonate derivative, and it was then used for the *O*-alkylation reaction with MTX.⁸ The product, MTX-linker **9**, was treated with TFA, yielding the MTX-linker **4**.

2.2. Design of PAMAM dendrimer conjugated with MTX through the photocleavable linker

In our photochemical approach to drug delivery, we chose a fifth generation (G5) PAMAM dendrimer (mean diameter ~ 5.4 nm⁴³) conjugated with a folic acid (FA) ligand as the cancer-targeting system that carries the photocaged MTX (Scheme 3). The notion that cancer cells are targetable by use of the folate ligand has been well established in the field of targeted delivery. Such cancer targeting relies on folate receptor (FAR)-mediated cellular uptake by a cancer cell with the up-regulated level of the folate receptor.^{5,6,23,44,45} Scheme 3 describes the synthesis of the dendrimer conjugate **11**, a FAR-targeting G5 PAMAM dendrimer conjugated with MTX through the photocleavable linker. First, a precursor dendrimer, G5-GA **10** (G5-glutaric acid; $M_n = 42730$ g mol⁻¹, PDI = $M_w/M_n \sim 1.046$),⁸ was preactivated by an EDC/NHS method, in which the carboxylic acid present on the dendrimer surface was converted to the amine-reactive *N*-hydroxysuccinimide ester. Second, the MTX-linker **4** and a FAR-targeting ligand (FA-ethylenediamine⁴⁶) were covalently coupled to the preactivated dendrimer through the amide formations. The dendrimer conjugate **11** was produced and purified by dialysis using membrane tubing (MWCO 10 kDa) to remove unreacted reactants and reagents. The purity of this conjugate **11** was determined by analytical HPLC ($\geq 96\%$), and its molar mass was determined by MALDI-TOF mass spectrometry (54,000 g mol⁻¹). The average number of the photocaged MTX and the FA ligands attached to the dendrimer was determined using the method described

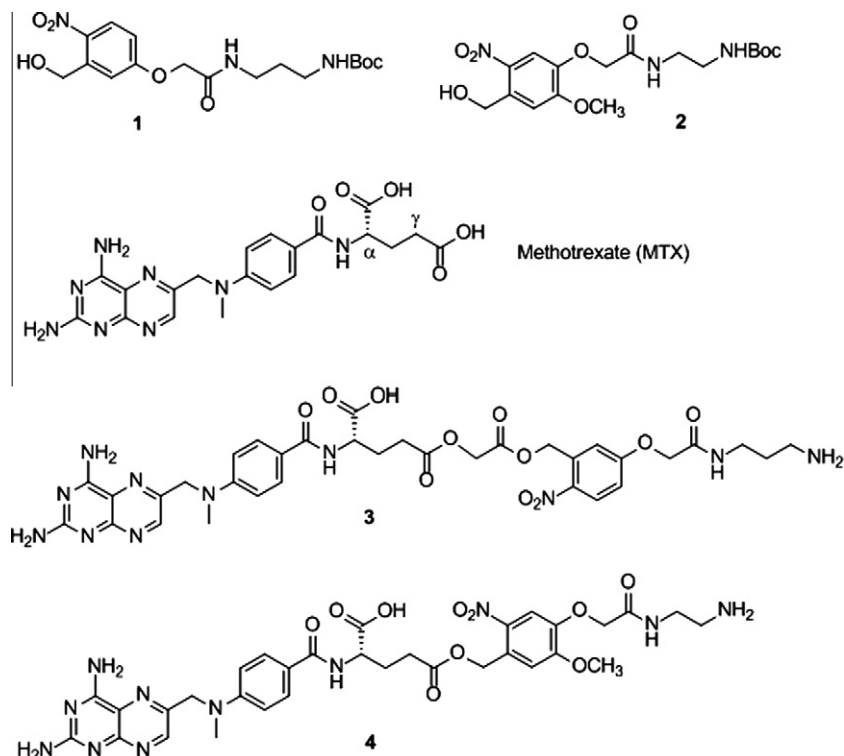
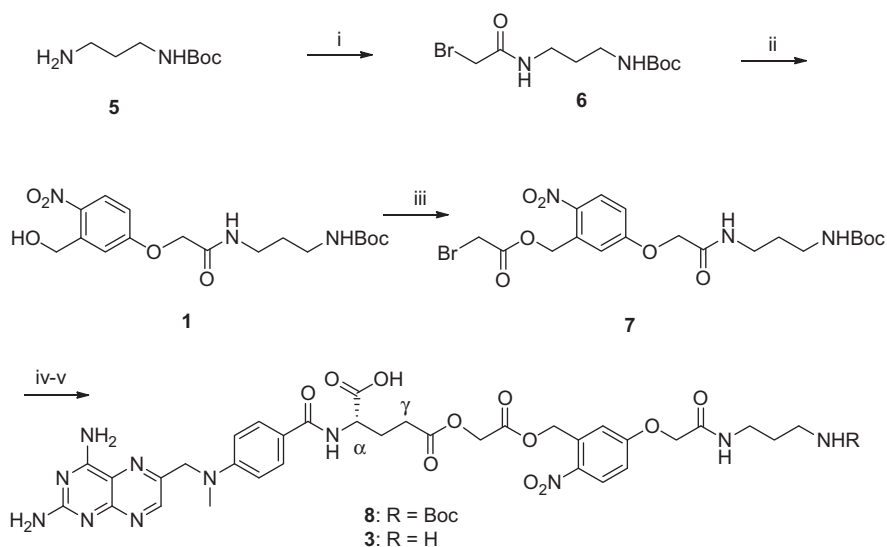


Figure 3. Structures of bifunctional *o*-nitrobenzyl (ONB) molecules **1**, **2** and two methotrexate (MTX)-ONB conjugates **3**, **4**, derived from the linkers.



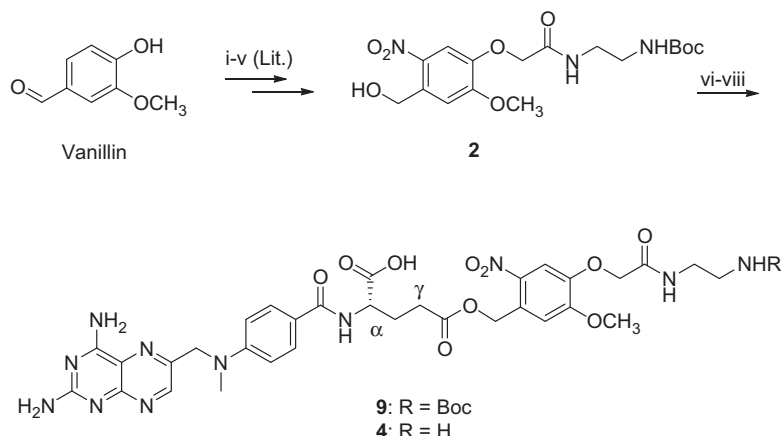
Scheme 1. Synthesis of a methotrexate (MTX)-ONB linker **3**. *Reagents and conditions:* (i) bromoacetyl chloride, *i*-Pr₂NEt, CH₂Cl₂, 0 °C; (ii) 2-nitro-5-hydroxybenzyl alcohol, K₂CO₃, MeCN, reflux; (iii) bromoacetyl chloride, *i*-Pr₂NEt, CH₂Cl₂, 0 °C to rt; (iv) methotrexate, Cs₂CO₃, DMF, rt, 24 h (23% isolation yield); (v) TFA, CH₂Cl₂, rt.

elsewhere^{8,25} after analysis of the data obtained from MALDI mass spectrometry,^{5,25} ¹H NMR spectroscopy,⁴⁷ and UV/vis spectrometry.^{8,25} The dendrimer conjugate **11** (G5-FA₄-MTX₈) contains on average four copies of the folate ligand and eight copies of **4** per dendrimer molecule.

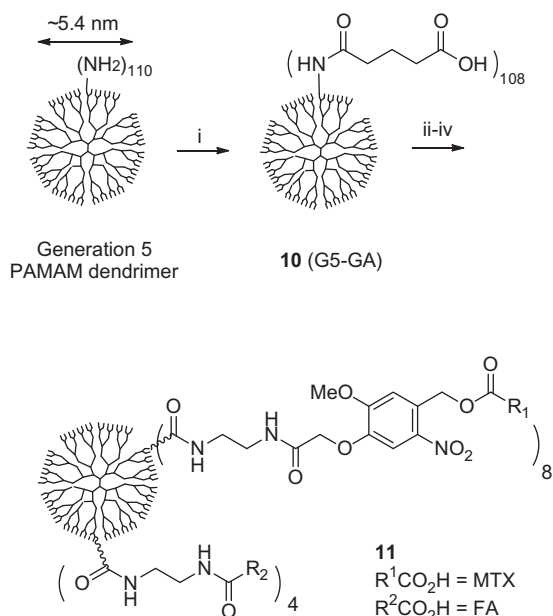
2.3. Photolysis of ONB linkers

The electronic absorption properties of the two ONB linkers **1** and **2** were studied by measuring their UV/vis absorption spectra in aqueous medium, as provided in Figure 4a. The linker **1** has λ_{\max}

at 310 nm ($\epsilon = 9575 \text{ M}^{-1} \text{ cm}^{-1}$), while the other linker, **2**, has λ_{\max} at the longer wavelength 340 nm ($\epsilon = 2750 \text{ M}^{-1} \text{ cm}^{-1}$). This spectral difference is attributable mainly to the effect of an additional methoxy group present at the ONB system **2**. Such a bathochromic shift is consistent with observations reported elsewhere^{48,49} that the addition of an electron-rich methoxy group into the ONB system leads to longer λ_{\max} and influences the quantum yield of ONB photolysis as well. The UV spectral data suggest such λ_{\max} of 310–340 nm as the preferred range of light that should provide an optimal level of photoactivation for the two ONB linkers or their MTX conjugates.



Scheme 2. Synthesis of a methotrexate (MTX)-ONB linker **4**. *Reagents and conditions:* (i) Ethyl bromoacetate, K_2CO_3 , DMF, rt; (ii) NaOH, THF, MeOH, H_2O , rt; (iii) concd HNO_3 , AcOH, 0°C to rt; (iv) *N*-Boc-1,2-diaminoethane, DCC, DMAP, DMF, 0°C to rt; (v) NaBH_4 , THF, MeOH, rt; (vi) methanesulfonyl chloride, Et_3N , CHCl_3 , 0°C to rt; (vii) Cs_2CO_3 , NaI, methotrexate, DMF, rt; (viii) TFA, CHCl_3 , rt, 15 min.



Scheme 3. Synthesis of a folate receptor-targeting PAMAM dendrimer conjugated with methotrexate (MTX) **11**. The dendrimer contains folic acid (FA) as the targeting ligand, and also carries MTX tethered at the photolabile ONB linker. *Reagents and conditions:* (i) glutaric anhydride, Et_3N , MeOH, rt, 24 h; (ii) NHS, EDC, DMAP, DMF, rt, 36 h; (iii) **4** (MTX-ONB linker, 15 mol eq per dendrimer), FA- $\text{CONHCH}_2\text{CH}_2\text{NH}_2$, 5 mol eq per dendrimer), Et_3N , DMF, rt, 36 h; (iv) ethanolamine; then dialysis (MWCO 10 kDa) against phosphate-buffered saline (PBS) and deionized water.

Photolysis of the two MTX-linker conjugates **3** and **4** was studied by exposing each conjugate dissolved in an aqueous solution ($30\ \mu\text{M}$) to the UV-A (365 nm) or UV-B (312 nm) light source. The UV/vis absorption spectra for each drug conjugate and its irradiation time course are shown in Figure 4b and c. Prior to irradiation, each MTX-linker conjugate shows strong absorption features at the range of a 250–400 nm wavelength, and such absorption results from the contribution of its ONB linker and MTX as well (Fig. 4a; absorption peaks: 310 nm, $\epsilon = 27535\ \text{M}^{-1}\ \text{cm}^{-1}$; 380 nm, $\epsilon = 7990\ \text{M}^{-1}\ \text{cm}^{-1}$). Following UV exposure, UV/vis absorption spectra were taken for each conjugate, and these showed significant changes in the absorption peaks that are assigned to the ONB linker. A rapid decrease in absorbance at around 310 nm was observed along with a concomitant increase at around

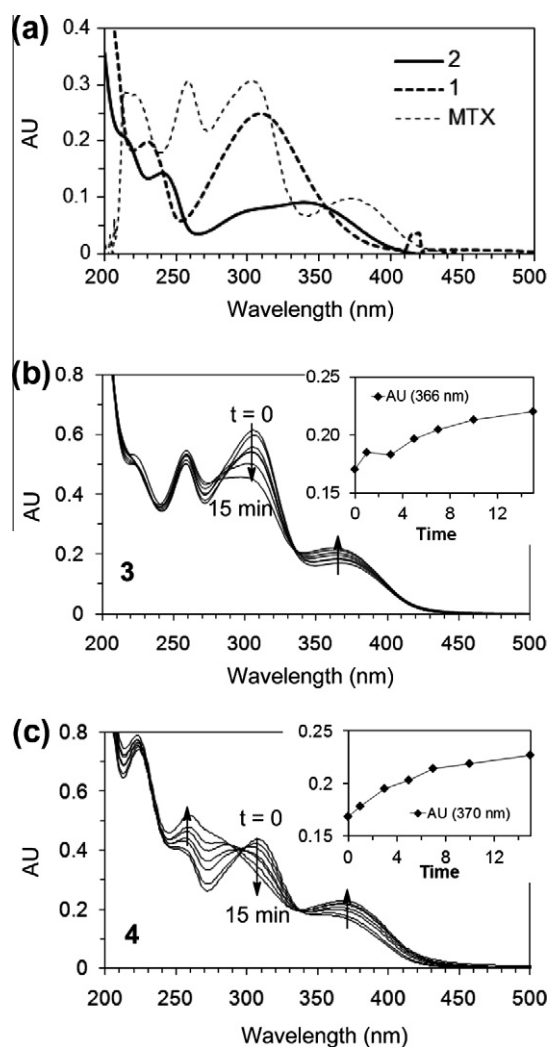


Figure 4. (a) UV/vis absorption spectra of methotrexate (MTX, $11\ \mu\text{M}$ in PBS), and two photocleavable linkers **1** ($26\ \mu\text{M}$) and **2** ($33\ \mu\text{M}$), each in an aqueous medium (0.5% MeOH/ H_2O); (b and c) UV/vis spectral traces of MTX-ONB conjugates **3** and **4** after exposure to UV-B (312 nm for **3**), or UV-A (365 nm for **4**) light as a function of irradiation time ($t = 0, 1, 3, 5, 7, 10, 15$ min). Each plot in the inset (b and c) shows the change in the absorption of the irradiated solution at the indicated wavelength that led to ONB-associated spectral changes.

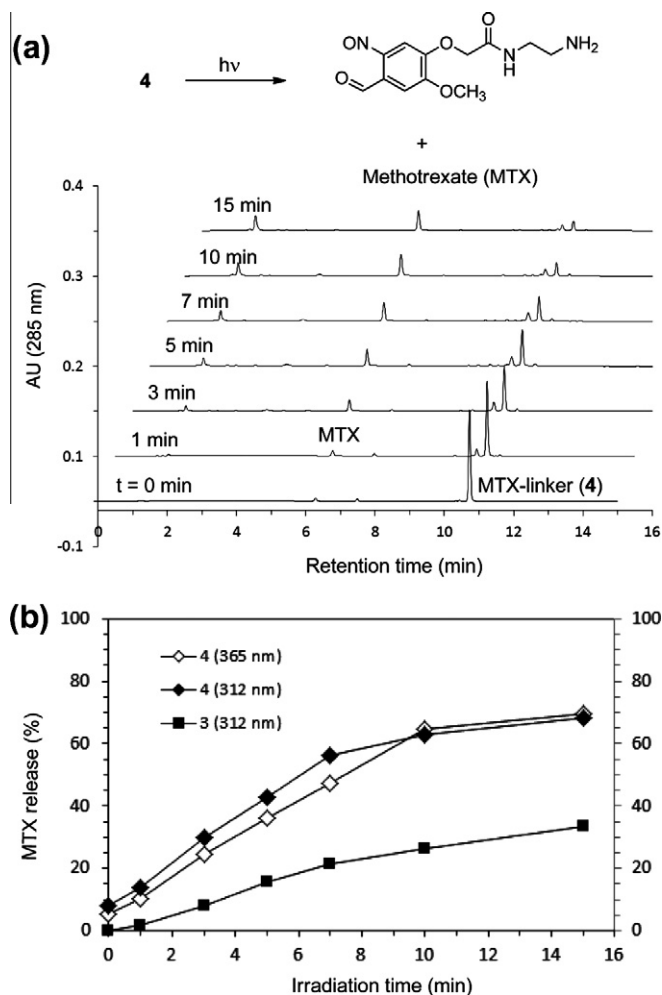


Figure 5. UV light-mediated release of methotrexate (MTX) from the MTX-ONB conjugate **4** ($30 \mu\text{M}$ in 2% MeOH/H₂O) by exposure to UV-A (365 nm) light. (a) HPLC traces of the irradiated solutions as a function of UV exposure time ($t = 0, 1, 3, 5, 7, 10, 15$ min); (b) plots for the photochemical release of MTX from MTX-ONB conjugates **3** and **4** as a function of time exposed to UV-B (312 nm) or UV-A (365 nm) light. In the release kinetics for **3** ($30 \mu\text{M}$ in 2% MeOH/H₂O), the drug release refers to the amount of MTX-glycolic acid.

370 nm. Such spectral features were reported similarly in the photolysis of the ONB linker **2** (quantum efficiency $\Phi = 0.29^8$). This spectral change is attributable to the photocleavage of the ONB linker, yielding a 2-nitrosobenzaldehyde-derived product, and as a consequence, triggering the MTX release. The UV/vis time course for each linker cleavage is illustrated by plotting the absorption at 366 or 370 nm as a function of irradiation time (inset). Each plot indicates faster increase in absorbance up to 7 min followed by slower increase. This spectrometric study suggests that the drug release occurs in a nonlinear manner and more rapidly in earlier time points.

The kinetics of the photochemical drug release for conjugate **4** was further investigated by using analytical reversed phase HPLC, as illustrated in Figure 5. HPLC traces acquired after UV exposure show growth of a peak assigned to the free MTX ($t_r = 6.1$ min) as a function of exposure time. The area under curve (AUC) for this peak was integrated to determine the percent amount of MTX released relative to the initial amount of **4**, and the rate of drug release is presented in Figure 5b. This figure also summarizes other release rates acquired from the MTX-linker conjugates **3** and **4** after UV exposure at 312 nm. The release results for **4** are characterized by several notable features that pertain to the kinetics of

linker photolysis. First, the drug release is time-dependent in a way that it was faster at early time points (up to 7 min). This result from the HPLC analysis is consistent with that from the earlier UV spectrophotometric analysis (Fig. 4). Second, the drug release is wavelength-dependent. The UV exposure at 312 nm led to a slightly faster release than at 365 nm before reaching a maximal level at 7–10 min. However, lack of a much larger difference between the two wavelengths might be attributable to the broad range of the absorptivity, from 300 to 370 nm, displayed by the photolinker **2** (Fig. 4a). Third, the drug release is linker-dependent, such that the efficiency of MTX release is greater for conjugate **4** than for conjugate **3**. Comparison of the two conjugates after maximal UV exposure (15 min) at 312 nm shows that **4** released MTX (68%) at the rate \sim two-fold greater than **3** (33%). In summary, we investigated a number of external and internal factors, including the linker structure, light wavelength, and irradiation time, and were able to understand the significance of the role played by each factor in photochemical drug release.^{48,49}

2.4. pH effect on linker photolysis

Our earlier investigation focused on the photochemical release of MTX performed at neutral pH. While certainly important, we also recognized that a study spanning a range of pHs was warranted given that pH clearly has physiological relevance in the development of targeted drug delivery strategies. For example, a tumor cell is characteristically more acidic than a normal healthy cell,⁵⁰ and subcellular compartments such as early endosomes and lysosomes where drug carriers are taken up and temporarily reside are acidic (pH <5–6) relative to the neutral cytosolic medium.^{51,52}

First, we performed photolysis experiments for the ONB linker **2** and determined whether the pH of the medium influenced the photocleavage rate (Fig. S1, Supplementary data). In this experiment, each photolytic reaction leads to the release of one water molecule ($R_1\text{OH} = \text{H}_2\text{O}$) per linker molecule⁴⁰ in a mechanism that involves the fragmentation of the ONB group to the nitrosobenzaldehyde derivative. The experiments were performed by exposure to longer wavelength light (365 nm), and the reaction progress after each exposure was monitored by ¹H NMR spectroscopy. Figure S1a illustrates a spectral region of interest selected for ¹H NMR spectra acquired for the photolysis of **2** in methanol-*d*₄ (1.2 mM) as a function of irradiation time. Proton signals H₃ and H₆, both assigned to the ONB aromatic system, decrease in their intensities. In addition, several new signals are generated over time as the photolysis products, including the aldehyde CH(=O) and its hydrate form CH(OH)₂. Integration of the area under each signal for the remaining **2** was quantified relative to an internal reference and was used to determine the rates of photolysis.

Figure S1b compares the time-courses for the photolytic reactions performed in various media. The result from methanol-*d*₄ shows that approximately 50% of the linker was cleaved within the 10-min period of irradiation. Notably, the results obtained from aqueous solutions performed at different pH conditions (pH 7.4, 9.0, and 5.0) show that the photolysis of **2** is significantly affected by the pH value of the medium. It is clear that the linker cleavage was faster at an acidic or basic solution than at the physiological condition (pH 7.4). The value of half-life $t_{1/2}$ (the exposure time required to afford 50% of linker cleavage) estimated from each curve allows us to summarize the order of the photolysis rate as follows: pH 9 (5 min) \geq pH 5 (8 min) > pH 7.4 (15 min). Such pH dependency observed in this NMR study is consistent with other observations that relate to the photolysis of ONB-tethered small molecules,⁴² including glycine⁵³ and urea.⁴⁸ We attribute the origin of this pH effect primarily to the photochemical mechanism that underlies the fragmentation of the ONB linker (Fig. 2). The

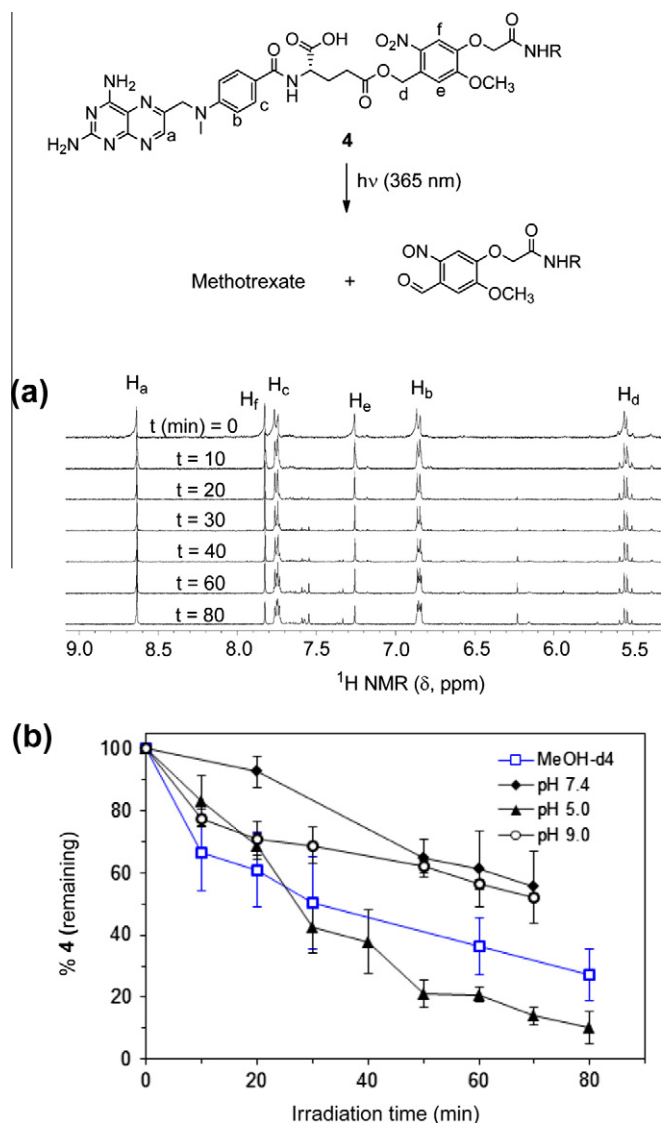


Figure 6. Photolysis of an ONB linker from the MTX-ONB conjugate **4** by exposure to UV-A light. (a) ¹H NMR spectral traces acquired after UV irradiation of **4** in MeOH-*d*₄ as a function of exposure time (*t* = 0–80 min); (b) pH effect on the rate of linker cleavage from **4** in the aqueous solution at pH 7.4 (50% CD₃CN/PBS), 9.0 (20% CD₃CN/D₂O), or 5.0 (20% CD₃CN/D₂O). The percent amount of intact **4** was determined by the peak integration method applied to the ONB-associated protons H_a, H_e, and H_f. Each data point represents a mean value from this analysis.

fragmentation mechanism is mediated by the formation of several charged species such as the *aci*-nitro form, and their rates of formation are likely to be sensitive to the pH variation.^{40,42}

2.5. pH effect on MTX release

We proceeded to determine whether the pH of the medium also influences the rate of drug release in lieu of water release, as studied earlier with the photolinker itself. This time, we studied the kinetics of the linker cleavage, using the MTX-linker conjugate **4** at variable pH conditions (Fig. 6). The progress of the reaction was monitored by ¹H NMR spectroscopy taken after exposure to the UV light. Figure 6a shows a spectral region of interest for the ¹H NMR spectra acquired from the experiments in methanol-*d*₄ (1.2 mM). Each spectral segment shows a subset of proton signals, including H_f, H_e, and H_b, that are assigned to the ONB linker. These ONB protons decrease in the peak intensities (and integration

areas) relative to an internal reference as a function of irradiation time. In addition to linker fragmentation, those proton signals assigned to MTX (H_b, H_c) split to more peaks in response to the irradiation, suggesting the release of free MTX molecules. The rate of MTX release acquired in methanol-*d*₄ is plotted in Figure 6b, showing that approximately 40% of the drug release is achieved within 30 min of irradiation. Such drug release of **4** occurs apparently more slowly than the cleavage of the linker **2**, as determined earlier (Fig. S1b). This lowered release rate is perhaps closely associated with the strong absorption of the applied UV light by the tethered drug molecule. The MTX molecule has strong absorption at 310–380 nm by its pteridine chromophore (Fig. 4a), and, therefore, the photoactivation of the ONB core might be competitively inhibited (Fig. 4c).

The kinetics of the drug release using the MTX-linker conjugate **4** (1.2 mM) was studied at variable pH conditions (7.4, 9.0, and 5.0), and the results are summarized in Figure 6b. Half life (*t*_{1/2}) for the drug release takes <30 min at pH 5, but is two-fold longer (≥70 min) at pH 7.4 or 9. In general, the release studies were performed at the mM concentration of **4**, and the rate was slower than that determined at a much lower concentration (30 μM) by the UV/vis and HPLC method (Fig. 5). In addition, this result diverges slightly from the pH trend we observed with the photolinker **2**, in which the rate of linker cleavage was almost similar at pH 5 and 9, but lower at pH 7.4 (Fig. S1). One reason for this difference may be the nature of the molecular species that is released as a result of the linker fragmentation. Upon photolysis, the ONB linker **2** releases the water molecule, but the MTX-ONB conjugate **4** releases MTX in a manner that its (L)-glutamyl carboxylic acid serves as the leaving group. Prior studies also showed mixed release profiles in response to pH variation that are dependent on the nature of the leaving group.^{53–55} Here, the release profile of MTX appears to correlate with the pH trend observed for glycine⁵³ or carbamylcholine⁵⁴ which was pH 5.5 > pH 9.0 > pH 7.4; it was not consistent with the release profile of *N*-methyl-*D*-aspartate⁵⁵

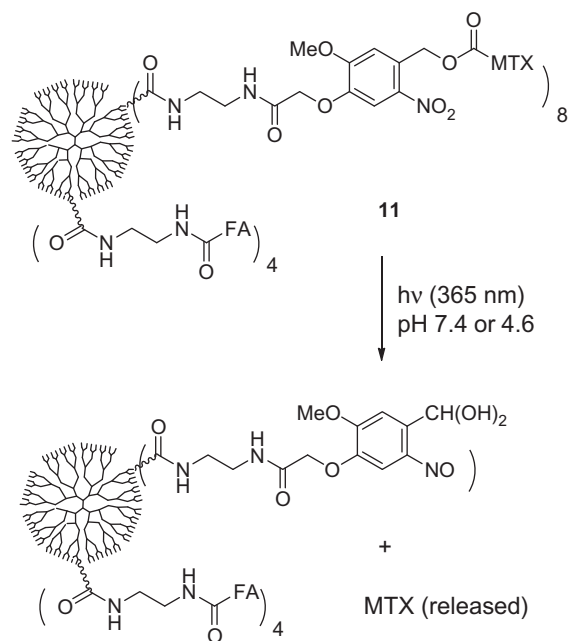


Figure 7. Light-controlled release of methotrexate (MTX) from **11**, a fifth generation PAMAM dendrimer conjugated with MTX through the photocleavable linker. The drug release was controlled by the irradiation of **11** (0.1 mg/mL, 1.96 μM) in the PBS buffer (pH 7.4), or acetate buffer (pH 4.6).

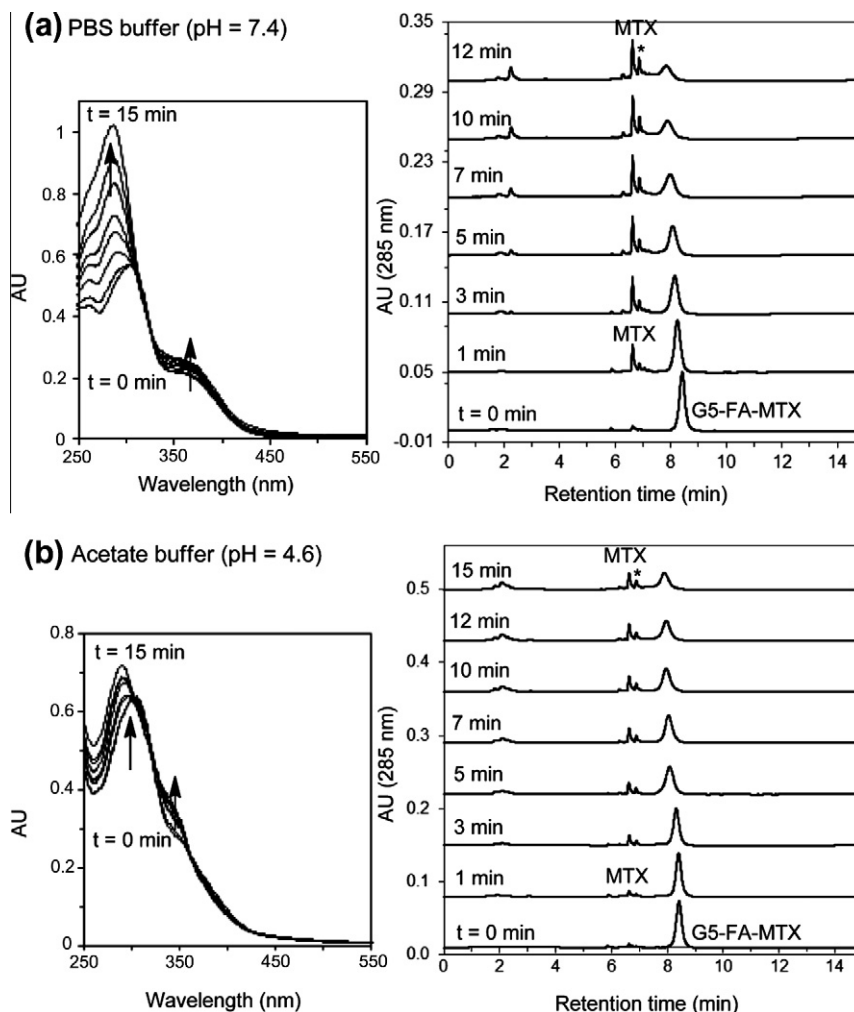


Figure 8. Photochemical MTX release from the dendrimer-MTX conjugate **11** (G5-FA₄-MTX₈). UV/vis spectra (left) and anal. HPLC traces (right) are shown for the release study performed at pH 7.4 (a) or 4.6 (b). Each spectral or chromatographic overlay is plotted as a function of UV exposure time ($t = 0$ –15 min). *This peak has an MTX-like UV/vis absorption profile, and its identity might be associated with MTX as the tautomer.

which was pH 4 > pH 7 > pH 10. Overall, the photochemical release of MTX is sensitive to pH variation.

2.6. MTX release from its PAMAM dendrimer conjugate

Light-controlled release of MTX was investigated with the ONB-linked MTX attached to PAMAM dendrimer (**11**, G5-FA₄-MTX₈) by exposing the dendrimer conjugate to UV-A light (Fig. 7). We studied the rate of drug release at two different pH conditions, 7.4 (PBS buffer) and 4.6 (acetate buffer). The progress of the release was monitored using a combination of UV/vis spectrometry and analytical HPLC, as illustrated in Figure 8. Conjugate **11** has a strong absorption features at 300–380 nm when measured in the PBS solution (Fig. 8a; see the UV/vis curve at $t = 0$ min). Such absorption features are attributable to a weighted combination of three independent chromophores comprising the folate ligand (280 nm, $\epsilon = 25545 \text{ M}^{-1} \text{ cm}^{-1}$; 347 nm, $\epsilon = 6676 \text{ M}^{-1} \text{ cm}^{-1}$), the MTX, and the ONB linker **2**. The UV/vis time course for the photolysis at pH 7.4 is characterized by large increases in the absorbance around 300 nm and small increases above 350 nm. The large increases were also observed in the photolysis of the MTX-linker conjugate **4** that lacks the FA ligand (Fig. 4c). The photolysis reaction performed at the acetate buffer (pH 4.6) led to smaller spectral changes at 280 and 350 nm (Fig. 8b). Thus, the rate of spectral changes suggests the contribution of the pH effect on the rate of drug release.

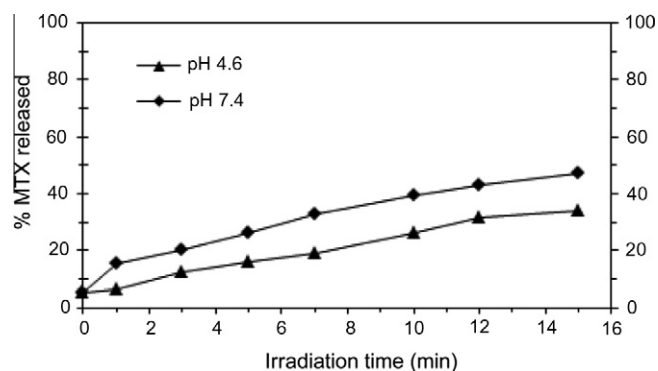


Figure 9. A summary for the amount of MTX released plotted as a function of exposure time at two different pH conditions. MTX was released from the dendrimer-MTX conjugate **11** by exposure to 365 nm light, and its amount was quantified by the AUC analysis for each of the HPLC traces shown in Figure 8.

We further determined the rate of MTX release by using the HPLC results, as illustrated with the overlaid HPLC traces (Fig. 8). The relative amount of MTX released was determined by the AUC method, and it is plotted as a function of UV exposure time (Fig. 9). At the end of the irradiation (15 min), the drug was

Table 1

A summary for the rate of drug (ligand) release at three different pH conditions.

Compound	Molecule released	$t_{1/2}$ (min) or relative rate ^a			
		MeOH	pH 5	pH 7.4	pH 9
2	H ₂ O	8	8	15	5
4	MTX	≤30	≤30	≥70	≥70
11	MTX	na	>15	15	na
Glycine (<i>N</i> -ONB) ⁵³	Glycine	na	+++	+	++
Carbamoylcholine (<i>N</i> -ONB) ⁵⁴	Carbamoylcholine	na	+++	+	++
NMDA (<i>O</i> -ONB) ⁵⁵	NMDA	na	+	++	++++

^a Relative order: ++++ (faster) to + (slower); na: not available.

released at 47% (pH 7.4) and 34% (pH 4.6). The results indicate a slightly faster release in the neutral condition from the PAMAM dendrimer conjugate **11**. This pH effect is the opposite of what we observed with the MTX-linker molecule **4**, where the drug release occurred faster under acidic conditions. These inconsistent trends suggest that there is no direct correlation between the MTX-release rate associated with the ONB-MTX molecule alone, and its much larger, dendrimer-tethered form. Table 1 compares photorelease profiles for various ONB-linked compounds studied here at various pH conditions along with the trends reported for other photocaged molecules^{53–55} in literature. The photolysis rates appear to be pH dependent, but such dependency also varies by the types of the compounds. This irregularity may be attributable to the differential contribution of multiple variables that include: (i) pH-dependent molar absorptivity (ϵ) of the ONB-linked drug conjugate (e.g., pH 7 > pH 5 in Figure 8); (ii) the leaving group (drug-released) effect^{53–55}; and (iii) the pH-responsive configurational changes of the PAMAM dendrimer.^{1,44} To our knowledge, such mechanistic aspects have not yet been thoroughly investigated, and remain to be better understood.

In summary, we demonstrated the photochemical mechanism of MTX release with the G5 PAMAM dendrimer conjugated with the photocaged MTX **11**. The drug release was achieved at both a neutral and an acidic condition, with a slightly greater rate at the neutral condition. One specific aspect of the photochemical applications we are currently interested in is to investigate the mechanism of drug action following cellular entry of nanoparticles conjugated with MTX. Despite extensive investigations of these nanoparticles as a delivery system to target cancer cells, the therapeutic action of these conjugates following cellular entry is poorly understood.^{1,5,17,28} In particular it is unclear whether the therapeutic activity requires release of the MTX. This light-controlled approach for the drug release will provide evidence whether MTX must be released to be fully able to inhibit the activity of its enzyme target DHFR (dihydrofolate reductase), and the growth of cancer cells. We will report the results of this application in due course.

3. Conclusion

The present study describes an ONB-based linker strategy for the light-controlled release of MTX. We demonstrated the release of MTX from both an ONB-tethered MTX molecule, and a folate receptor-targeting PAMAM dendrimer carrying the photocaged drug. Certain factors are considered to be important for controlling the drug release, including light wavelengths, exposure time, the substitution patterns of the photolabile ONB core, and the pH values of the media where the drug release occurs. In this study, we demonstrated that UV light serves as an effective trigger mechanism, and it could be applied in an active manner orthogonal to other passive release approaches. We believe that this photochemical approach is generally applicable for other anticancer drugs and other

delivery applications in vitro or perhaps in vivo—in particular, those therapeutic and diagnostic applications that require non-invasive or spatiotemporal drug/probe activation.

4. Materials and methods

General synthetic methods, details of synthesis (**1–4**), and copies of their spectral data are provided in the Supplementary data.

4.1. Synthesis of PAMAM dendrimer conjugate **11** (Scheme 3)

Generation 5 PAMAM dendrimer was purchased as a 17.5% (wt/wt) methanol solution (Dendritech, Inc., Midland, MI), and purified by dialysis (MWCO 10 kDa) prior to use as described elsewhere.^{5, 8,25, 47} The average number of primary amines per dendrimer molecule ($\#NH_2$ per dendrimer \approx 110) was determined by potentiometric titration.⁵ Glutaric acid-derivatized dendrimer **10** was prepared as described earlier.^{8,25} The average number of glutaric acid molecules attached on the surface was determined by the NMR method (Supplementary data, page S16) where the integration area for the proton signals of glutaric acid was compared to that of select dendrimer protons.

Preparation of a fifth generation PAMAM dendrimer conjugated with folic acid and MTX **11** was performed according to the dendrimer conjugation method described elsewhere.^{8,25} First, the glutaric acid-derivatized dendrimer **10** (25 mg) was activated to its NHS ester form by treatment with 4-dimethylaminopyridine (9 mg, 73.8 μ mol), *N*-hydroxysuccinimide (9 mg, 78.2 μ mol), and 1-ethyl-3-(3-dimethylaminopropyl)carbodiimide hydrochloride (15 mg, 78.2 μ mol) in anhydrous DMF (10 mL) at rt. After preactivation for 36 h at rt, FA-ethylnediamine⁴⁶ (**10**; 1.5 mg, 3.0 μ mol), **4**-TFA salt (9.2 μ mol), and triethylamine (4.3 μ L, 30.9 μ mol), each dissolved in a minimal volume of DMF, were added to the preactivated dendrimer solution. After stirring at rt for 36 h in the dark, the reaction mixture was treated with ethanolamine (7.4 μ L, 123 μ mol). After stirring for additional 2 h, the conjugation reaction was quenched by adding water (2 mL), and the mixture was concentrated in vacuo. The residue was diluted with water (15 mL) and dialyzed by using membrane tubing (MWCO 10 kDa, Spectrum[®] Labs, Inc.) against deionized water (4 L), a phosphate-buffered saline solution (1 \times 4 L), and deionized water (3 \times 4 L) over 3 days. The dialyzed solution contained in the tubing was collected and lyophilized, yielding **11** as pale yellow fluffy solid (19 mg). ¹H NMR (400 MHz, D₂O/DMSO-*d*₆): δ = 8.55 (br), 8.46 (s), 8.0–7.8 (br m), 7.60 (m), 7.55 (br), 7.05 (br), 6.70 (br m), 6.55 (br), 6.41 (br), 5.35 (br), 3.30 (m), 3.20–3.0 (br s), 2.7–2.5 (br m), 2.40–2.30 (br), 2.20–2.0 (br m), 1.60 (br) ppm. The number ratio between FA and MTX attached per dendrimer was determined by the analysis of ¹H NMR signals for FA and MTX (δ = 8.46, 6.7 ppm, respectively) and for the *ortho*-nitrobenzyl linker (δ = 7.05, 5.35 ppm): the ratio = [(number of MTX) \div (number of FA)] = $N_{MTX} \div N_{FA}$ = 2.1]. An average molecular weight of **11** was

determined by MALDI TOF on the basis of a peak intensity at $m/z = 54000 \text{ gmol}^{-1}$. Increment in the molecular weight of **11** relative to **10** ($m/z = 40200 \text{ gmol}^{-1}$)⁸ is attributed to the molecular weight contributed from both FA, MTX, and hydroxyethylamine (HEA) attached to **10**: $\Delta \text{wt (unit, gmol}^{-1}) = [54000 (\mathbf{11}) - 40200 (\mathbf{10}) - 5800 (\text{HEA})] = 8000 = [(MW_{\text{of FA}}) \times N_{\text{FA}} + (MW_{\text{of 4}}) \times N_{\text{MTX}}] = [483 \times N_{\text{FA}} + 735 \times N_{\text{MTX}}]$. The mean number for FA and MTX attached per dendrimer was thus calculated by solving the two equations: 4.1 (FA) and 8.2 (MTX).

4.2. Photolysis experiments of **3** and **4** (Figs. 4 and 5)

Photolysis experiments were carried out using Spectroline® UV bench lamps (XX-15A; power = 1.1 mW/cm²), either at the UV-B (312 nm) or UV-A (365 nm) wavelength. As a representative photolysis method, the linker **3** was dissolved in an aqueous medium (30 μM, 2% MeOH/H₂O), and the solution (20 mL) was loaded onto a glass Petri dish. The linker solution was exposed to the UV lamps irradiated at the distance of ~5 cm at 312 nm over up to 15 min. Progress of the photolysis was monitored by UV/vis spectrometry, and for the analysis, each aliquot (700 μL) was taken out during the exposure at a specific time point as indicated in Figure 4. Photolysis of the linker **4** was performed similarly in the same aqueous medium (30 μM) at 312 or 365 nm, and its reaction aliquots were analyzed by both the UV/vis (Fig. 4) and analytical HPLC method (Fig. 5).

4.3. Photolysis experiments of **2** (Fig. S1)

Stock solutions for the photolysis of the linker **2** (1.2 mM) were prepared in deuterated methanol (CD₃OD), or the pH-adjusted deuterated aqueous media that include 50% CD₃CN/PBS (pH 7.4), 20% CD₃CN/D₂O (pH 9.0), and 20% CD₃CN/D₂O (pH 5.0). Each of the sample solutions (0.5 mL) was loaded in an NMR sample tube, and exposed to UV light at 365 nm for up to 30 min as indicated in Figure S1. Progress of the linker cleavage was monitored by ¹H NMR spectroscopy as illustrated in Figure S1a. Addition of deuterated acetonitrile as a co-solvent was to increase the aqueous solubility of the linker and also to use it as an internal reference for calculating the integration area for each peak of interest. The amount of the linker **2** that remained intact was quantified by analyzing integration areas for selected proton signals such as aromatic protons (H₃, H₆), methoxy (OCH₃), and benzylic (PhCH₂OH) protons. Each data point represents a mean value acquired from the experiments performed in duplicate.

4.4. Photolysis experiments of **4** (Fig. 6)

The stock solution for the photolysis of MTX-linker **4** (1.2 mM) was prepared in deuterated methanol (CD₃OD), or the pH-adjusted deuterated water (D₂O) as described earlier. Each of the solutions (0.5 mL) was loaded into an NMR sample tube, and irradiated at 365 nm for up to 80 min as indicated in Figure 6. Progress of the photochemical drug release was monitored by ¹H NMR spectroscopy as illustrated in Figure 6a. The amount of the MTX-linker **4** that remained intact was quantified by analysis of the integration area for each of the protons H_d, H_e, and H_f.

4.5. Photolysis of dendrimer-MTX conjugate **11G5-FA₄-MTX₈** (Figs. 7 and 8)

An aqueous solution of **11** (0.1 mg/mL, 1.85 μM) was prepared in a PBS buffer solution (pH 7.4), and also separately in an acetate buffer (pH 4.65). Each solution (20 mL) was loaded in a glass Petri dish, placed under UV lamps at the distance of ~5 cm, and exposed at 365 nm over up to 15 min. Progress of the drug release was

monitored by UV/vis spectrometry. The analytical HPLC was also performed for each aliquot (700 μL) which was taken out at a specific time point as indicated in Figure 8.

Acknowledgments

This work was supported by the National Cancer Institute, National Institutes of Health under award 1 R01 CA119409. The author (S.K.C.) thanks Undergraduate Research Opportunity Program (UROP) at University of Michigan for its support, and also for the UROP fellowship (J.S.). We thank Mr. Ankur Desai for his help in the HPLC analysis.

A. Supplementary data

Supplementary data (A full description of synthetic details for compounds **1–4**, copies of their ¹H NMR, and mass spectra, full ¹H NMR spectral traces for Figure S1 and 76, and copies of GPC and MALDI TOF traces for **10–11**.) associated with this article can be found, in the online version, at doi:10.1016/j.bmc.2011.12.020.

References and notes

1. Majoros, I. J.; Williams, C. R.; Becker, A.; Baker, J. R., Jr. *WIREs: Nanomed. Nanobiotech.* **2009**, *1*, 502.
2. Svenson, S. *Eur. J. Pharm. Biopharm.* **2009**, *71*, 445.
3. Brigger, I.; Dubernet, C.; Couvreur, P. *Adv. Drug Delivery Rev.* **2002**, *54*, 631.
4. Ojima, I. *Acc. Chem. Res.* **2008**, *41*, 108.
5. Majoros, I. J.; Thomas, T. P.; Mehta, C. B.; Baker, J. R., Jr. *J. Med. Chem.* **2005**, *48*, 5892.
6. Feazell, R. P.; Nakayama-Ratchford, N.; Dai, H.; Lippard, S. J. *J. Am. Chem. Soc.* **2007**, *129*, 8438.
7. Dubowchik, G. M.; Walker, M. A. *Pharmacol. Ther.* **1999**, *83*, 67.
8. Choi, S. K.; Thomas, T.; Li, M.; Kotlyar, A.; Desai, A.; Baker, J. R., Jr. *Chem. Commun.* **2010**, 2632.
9. Shamay, Y.; Adar, L.; Ashkenasy, G.; David, A. *Biomaterials* **2011**, *32*, 1377.
10. Johnson, J. A.; Lu, Y. Y.; Burts, A. O.; Xia, Y.; Durrell, A. C.; Tirrell, D. A.; Grubbs, R. H. *Macromolecules* **2010**, *43*, 10326.
11. Agasti, S. S.; Chompoosor, A.; You, C.-C.; Ghosh, P.; Kim, C. K.; Rotello, V. M. *J. Am. Chem. Soc.* **2009**, *131*, 5728.
12. Lin, Q.; Huang, Q.; Li, C.; Bao, C.; Liu, Z.; Li, F.; Zhu, L. *J. Am. Chem. Soc.* **2010**, *132*, 10645.
13. McCoy, C. P.; Rooney, C.; Edwards, C. R.; Jones, D. S.; Gorman, S. P. *J. Am. Chem. Soc.* **2007**, *129*, 9572.
14. Rapoport, N.; Gao, Z.; Kennedy, A. J. *Natl. Cancer Inst.* **2007**, *99*, 1095.
15. Pitt, W. G.; Hussein, G. A.; Staples, B. J. *Expert Opin. Drug Deliv.* **2004**, *1*, 37.
16. Williams, J. W.; Morrison, J. F.; Duggleby, R. G. *Biochemistry* **2002**, *18*, 2567.
17. Kukowska-Latallo, J. F.; Candido, K. A.; Cao, Z.; Nigavekar, S. S.; Majoros, I. J.; Thomas, T. P.; Balogh, L. P.; Khan, M. K.; Baker, J. R., Jr. *Cancer Res.* **2005**, *65*, 5317.
18. Schnell, J. R.; Dyson, H. J.; Wright, P. E. *Annu. Rev. Biophys. Biomol. Struct.* **2004**, *33*, 119.
19. Mauldin, R. V.; Carroll, M. J.; Lee, A. L. *Structure* **2009**, *17*, 386.
20. Huang, X.; Du, F.; Ju, R.; Li, Z. *Macromol. Rapid Commun.* **2007**, *28*, 597.
21. Dendooven, A.; De Rycke, L.; Verhelst, X.; Mielants, H.; Veys, E. M.; De Keyser, F. *Ann. Rheum. Dis.* **2006**, *65*, 833.
22. Majoros, I. J.; Williams, C. R.; James, R.; Baker, J. *Curr. Topics Med. Chem.* **2008**, *8*, 1165.
23. Majoros, I. J.; Myc, A.; Thomas, T.; Mehta, C. B.; Baker, J. R. *Biomacromolecules* **2006**, *7*, 572.
24. Hong, S.; Leroueil, P. R.; Majoros, I. J.; Orr, B. G.; Baker, J. R., Jr.; Banaszak Holl, M. M. *Chem. Biol.* **2007**, *14*, 107.
25. Thomas, T. P.; Choi, S. K.; Li, M.-H.; Kotlyar, A.; Baker, J. R., Jr. *Bioorg. Med. Chem. Lett.* **2010**, *20*, 5191.
26. Tassa, C.; Duffner, J. L.; Lewis, T. A.; Weissleder, R.; Schreiber, S. L.; Koehler, A. N.; Shaw, S. Y. *Bioconjugate Chem.* **2010**, *21*, 14.
27. Mammen, M.; Choi, S. K.; Whitesides, G. M. *Angew. Chem. Int. Ed.* **1998**, *37*, 2754.
28. Thomas, T. P.; Majoros, I. J.; Kotlyar, A.; Kukowska-Latallo, J. F.; Bielinska, A.; Myc, A.; Baker, J. R., Jr. *J. Med. Chem.* **2005**, *48*, 3729.
29. Etrych, T.; Mrkván, T.; Říhová, B.; Ulbricht, K. J. *Controlled Release* **2007**, *122*, 31.
30. Lee, R. J.; Low, P. S. *Biochim. Biophys. Acta (BBA)—Biomembranes* **1995**, *1233*, 134.
31. Huang, B.; Tang, S.; Desai, A.; Cheng, X.-m.; Kotlyar, A.; Spek, A. V. D.; Thomas, T. P.; Baker, J. R., Jr. *Bioorg. Med. Chem. Lett.* **2009**, *19*, 5016.
32. Naughton, D. P. *Adv. Drug Delivery Rev.* **2001**, *53*, 229.
33. Mayer, G.; Heckel, A. *Angew. Chem. Int. Ed.* **2006**, *45*, 4900.
34. Lemke, E. A.; Summerer, D.; Geierstanger, B. H.; Brittain, S. M.; Schultz, P. G. *Nature Chem. Biol.* **2007**, *3*, 769.

35. Goard, M.; Aakalu, G.; Fedoryak, O. D.; Quinonez, C.; St. Julien, J.; Poteet, S. J.; Schuman, E. M.; Dore, T. M. *Chem. Biol.* **2005**, *12*, 685.
36. Furuta, T.; Wang, S. S. H.; Dantzker, J. L.; Dore, T. M.; Bybee, W. J.; Callaway, E. M.; Denk, W.; Tsien, R. Y. *Proc. Natl. Acad. Sci. U.S.A.* **1999**, *96*, 1193.
37. Neveu, P.; Aujard, I.; Benbrahim, C.; Le Saux, T.; Allemand, J.-F.; Vriz, S.; Bensimon, D.; Jullien, L. *Angew. Chem. Intl. Ed.* **2008**, *47*, 3744.
38. Du, H.; Boyd, M. K. *Tetrahedron Lett.* **2001**, *42*, 6645.
39. Qvit, N.; Monderer-Rothkoff, G.; Ido, A.; Shalev, D. E.; Amster-Choder, O.; Gilon, C. *Peptide Sci.* **2008**, *90*, 526.
40. Gaplovsky, M.; Il'ichev, Y. V.; Kamdzhilov, Y.; Kombarova, S. V.; Mac, M.; Schworer, M. A.; Wirz, J. *Photochem. Photobiol. Sci.* **2005**, *4*, 33.
41. Cummings, R. T.; Krafft, G. A. *Tetrahedron Lett.* **1988**, *29*, 65.
42. Il'ichev, Y. V.; Schwörer, M. A.; Wirz, J. *J. Am. Chem. Soc.* **2004**, *126*, 4581.
43. Tomalia, D. A.; Naylor, A. M.; William, A.; Goddard, I. *Angew. Chem. Intl. Ed.* **1990**, *29*, 138.
44. Majoros, I.; Baker, J., Jr. *Dendrimer-Based Nanomedicine*; Pan Stanford: Hackensack, NJ, 2008. p. 436.
45. Low, P. S.; Henne, W. A.; Doorneweerd, D. D. *Acc. Chem. Res.* **2008**, *41*, 120.
46. Whiteley, J. M.; Henderson, G. B.; Russell, A.; Singh, P.; Zevely, E. M. *Anal. Biochem.* **1977**, *79*, 42.
47. Choi, S. K.; Leroueil, P.; Li, M.-H.; Desai, A.; Zong, H.; Van Der Spek, A. F. L.; Baker, J. R., Jr. *Macromolecules* **2011**, *44*, 4026.
48. Wilcox, M.; Viola, R. W.; Johnson, K. W.; Billington, A. P.; Carpenter, B. K.; McCray, J. A.; Guzikowski, A. P.; Hess, G. P. *J. Org. Chem.* **1990**, *55*, 1585.
49. Katritzky, A. R.; Xu, Y.-J.; Vakulenko, A. V.; Wilcox, A. L.; Bley, K. R. *J. Org. Chem.* **2003**, *68*, 9100.
50. Tannock, I. F.; Rotin, D. *Cancer Res.* **1989**, *49*, 4373.
51. Lee, R. J.; Wang, S.; Low, P. S. *Biochim. Biophys. Acta (BBA)—Mol. Cell. Res.* **1996**, *237*.
52. Murphy, R. F.; Powers, S.; Cantor, C. R. *J. Cell Biol.* **1984**, *98*, 1757.
53. Billington, A. P.; Walstrom, K. M.; Ramesh, D.; Guzikowski, A. P.; Carpenter, B. K.; Hess, G. P. *Biochemistry* **1992**, *31*, 5500.
54. Walker, J. W.; McCray, J. A.; Hess, G. P. *Biochemistry* **1986**, *25*, 1799.
55. Gee, K. R.; Niu, L.; Schaper, K.; Jayaraman, V.; Hess, G. P. *Biochemistry* **1999**, *38*, 3140.